REPORT DOCUMENTATION PAGE

Form Approved
OMB No. 0704-0188

1. REPORT DATE *(DD-MM-YYYY)*	**2. REPORT TYPE**	**3. DATES COVERED** *(From - To)*
16-03-2007	Technical Paper	

4. TITLE AND SUBTITLE

Atomization Performance Predictions of Gas-Centered Swirl-Coaxial Injectors

5a. CONTRACT NUMBER

5b. GRANT NUMBER

5c. PROGRAM ELEMENT NUMBER

6. AUTHOR(S)
Malissa D.A. Lightfoot, Stephen A. Danczyk, and Douglas G. Talley

5d. PROJECT NUMBER
50260538

5e. TASK NUMBER

5f. WORK UNIT NUMBER

7. PERFORMING ORGANIZATION NAME(S) AND ADDRESS(ES)

Air Force Research Laboratory (AFMC)
AFRL/PRSA
10 E. Saturn Blvd.
Edwards AFB CA 93524-7680

8. PERFORMING ORGANIZATION REPORT NUMBER

AFRL-PR-ED-TP-2007-121

9. SPONSORING / MONITORING AGENCY NAME(S) AND ADDRESS(ES)

Air Force Research Laboratory (AFMC)
AFRL/PRS
5 Pollux Drive
Edwards AFB CA 93524-70448

10. SPONSOR/MONITOR'S ACRONYM(S)

11. SPONSOR/MONITOR'S NUMBER(S)
AFRL-PR-ED-TP-2007-121

12. DISTRIBUTION / AVAILABILITY STATEMENT

Approved for public release; distribution unlimited (Public Affairs No. 07113A).

13. SUPPLEMENTARY NOTES
EXPORT CONTROL. Presented at the JANNAF 54th Propulsion Meeting/3rd Liquid Propulsion Subcommittee/2nd Spacecraft Propulsion Subcommittee/5th Modeling and Simulation Subcommittee Joint Meeting, Denver, CO, 14-17 May 2007.

14. ABSTRACT

The ability to predict injector performance can reduce the cost of rocket engine development. This paper details a new theory to predict the atomization efficiency and droplet diameter from the atomization of wall-bounded films with strong gas-phase influences. In this theory atomization occurs when a disturbance is created on the film surface then breaks down into droplets via stripping. The theory relates the mass of film lost via atomization to the mass of liquid introduced into the atomizer to predict atomization efficiency and offers some estimations of primary droplet diameter. A specific example involving a gas-centered swirl coaxial injector is discussed. The results of experiments and simulations are used to support assumptions and are successfully compared to some simple predictions from the theory. Despite the application to a specific injector efforts are made to keep the theory as general as possible so that it applies to many types of injectors and a wide range of operating conditions.

15. SUBJECT TERMS

16. SECURITY CLASSIFICATION OF:			**17. LIMITATION OF ABSTRACT**	**18. NUMBER OF PAGES**	**19a. NAME OF RESPONSIBLE PERSON**
					Dr. Stephen A. Danczyk
a. REPORT	**b. ABSTRACT**	**c. THIS PAGE**	SAR	10	**19b. TELEPHONE NUMBER** *(include area code)* N/A
Unclassified	**Unclassified**	**Unclassified**			

Atomization Performance Predictions of Gas-Centered Swirl-Coaxial Injectors

Malissa D.A. Lightfoot, Stephen A. Danczyk and Douglas G. Talley
Air Force Research Laboratory
Edwards AFB, CA

ABSTRACT

The ability to predict injector performance can reduce the cost of rocket engine development. This paper details a new theory to predict the atomization efficiency and droplet diameter from the atomization of wall-bounded films with strong gas-phase influences. In this theory atomization occurs when a disturbance is created on the film surface then breaks down into droplets via stripping. The theory relates the mass of film lost via atomization to the mass of liquid introduced into the atomizer to predict atomization efficiency and offers some estimations of primary droplet diameter. A specific example involving a gas-centered swirl coaxial injector is discussed. The results of experiments and simulations are used to support assumptions and are successfully compared to some simple predictions from the theory. Despite the application to a specific injector efforts are made to keep the theory as general as possible so that it applies to many types of injectors and a wide range of operating conditions.

INTRODUCTION AND BACKGROUND

INTRODUCTION

The introduction of liquid and its atomization are important subprocesses in the operation of a rocket engine. Understanding the atomization process is important for predicting not only the efficiency of the engine but also its stability. Atomization is generally viewed as a device-dependent operation, i.e. atomization quality and character depends on the specific type of injector. A recent review of the mechanisms effecting atomization[1] brings to light a device-independent view, however. Here a theory is presented that leverages this more general approach. Because the theory is rooted in general mechanisms, only small changes are necessary to apply it to a variety of injectors.

This work was motivated by studies of a specific injector—a gas-centered swirl-coaxial (GCSC) injector. Application of the theory to this type of injector is considered here. A schematic of the injector is shown in Fig. 1. Liquid is injected tangentially along the outer wall of the injector. This tangential injection causes a swirling film to form along the wall. High-speed, nonswirling gas is introduced axially through the center of the injector. This injector is an effective atomizer because the gas is at a much higher speed than the liquid and, therefore, the gas momentum flux is larger than the liquid momentum flux. These injectors are similar to other injectors such as pressure-swirl and coaxial air-blast atomizers, except they do not produce a conical sheet at typical rocket engine operating conditions[2, 3]. Instead, most of the atomization occurs from a wall-bounded film inside the injector cup[3]. Little work exists to describe or predict atomization of wall-bound films, particularly at the injection velocities and pressures found in rocket engine operation.

Earlier work considered various atomization mechanisms and identified those most likely at work in GCSC injectors[1]. Numerical and experimental testing further reinforced these identifications[4]. As a consequence of these findings, the theory developed here assumes atomization results from the stripping of mass off of various disturbances. These disturbances may be caused by hydrodynamic instability, turbulence or large-scale gas-phase structures (such as recirculation zones). The current work describes the stripping process and develops an approach for calculating the rate of atomization and primary droplet size. The keystone of this theory is the assumption that atomization occurs when the forces on a section of the film are balanced. Following the presentation of the general theory, specifics related to applying it to GSCS injectors are

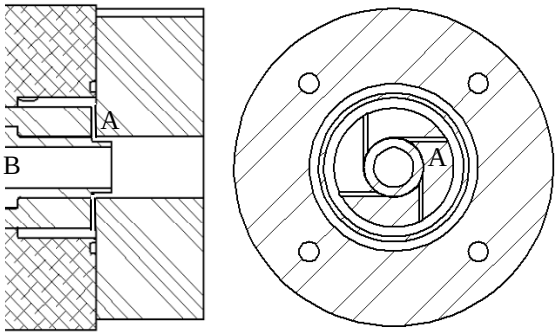

Figure 1. Partial schematic of the experimental apparatus. The liquid enters through the tubes labeled A; gas enters at B. The gas inlet extends beyond what is pictured.

given. The application section particularly focuses on the type of disturbances likely to be important at usual operating conditions. Simplifications and assumptions are also discussed. In the applied section, experimental and numerical results are referenced in support of various findings. These results are currently of limited scope, but demonstrate the promise of the theory. The set-up of the experiments and simulations are briefly described below.

EXPERIMENTAL AND NUMERICAL SIMULATION BACKGROUND

NUMERICAL SIMULATIONS

Computational fluid dynamics simulations were performed using FLUENT 6.2 software. The axisymmetric geometry for the simulations is given in Fig. 2. Even with an axisymmetric solution, tangential velocities were considered with swirl added as a percentage of the total mass flow in the inlet conditions. A quadrilateral grid was used. Grid points were clustered around the expected interface location. FLUENT tracks the interface using a VOF method with a piece-wise linear reconstruction. A realizable k-ε turbulence model was used for these initial results. Fully resolving this flow requires an extremely large number of grid points (10's to 100's of millions) due to the sharp gradients created by the existence of a gas-liquid interface and the small size of the droplets produced. Despite the lack of complete resolution, the numerical results give qualitative insight and suggest trends, the confirmation of which has been seen experimentally.

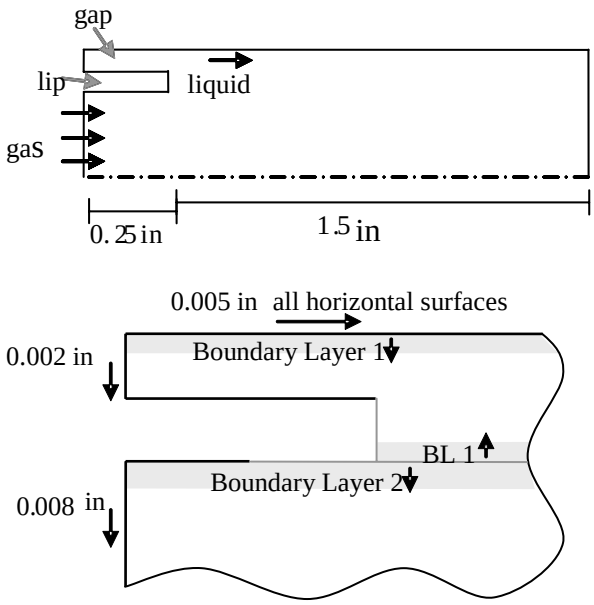

Figure 2. Axisymmetric slice of a gas-centered coaxial-swirl injector with grid spacing shown below. The gap is 0.06 in high, the lip is 0.065 in high and the gas inlet has a radius of 0.25 in. Boundary layer (BL) 1 starts at 0.005 in and grows at a rate of 0.9091 while Boundary Layer 2 starts at 0.0055 in and grows at a rate of 1.1.

A steady, single-phase solution was developed for the gas by treating the fuel inlet as a wall. The gas inlet condition was fully developed pipe flow at a set mass flow rate, also calculated using FLUENT. The outlet was treated as a constant-pressure boundary at atmospheric pressure; atmospheric pressure was chosen because the complimentary experiments were carried out at that pressure. This gas-phase solution was used as the initial solution for the two-phase simulation.

EXPERIMENTAL SET-UP

Atmospheric tests were conducted with an injector with the geometry shown in Figs. 1 and 2. This geometry is the same as that used in the simulations with the addition of a longer gas inlet post. The outlet section of the injector, where the liquid and gas come into contact, was constructed of plexiglass to enable imaging of the film. The remainder of the injector was constructed of stainless steel. The design is modular allowing various geometric parameters to be easily altered by replacing individual sections of the assembly. To help minimize aberrations and other problems associated with filming through curved surfaces, four flat "viewing windows" were cut into the outlet section of the injector.

The chamber in which the tests were run is essentially a plexiglass box. Two sides of the box have access holes several centimeters high and the width of the box along their top edges. These access holes allow access to the injector during and between runs. The bottom of the chamber has a diffuser to minimize splashing, a drain for the water and side vents through which nitrogen is drawn at a low velocity. These vents help to draw small droplets down and out of the chamber so that it does not fill with mist.

The operating fluids were gaseous nitrogen and water. The main diagnostics for these tests were backlit photographs taken with a digital camera and high speed video taken with a Phantom high speed

camera. The viewing windows were kept clear with gas curtains using nitrogen. The curvature of the injector focuses the backlight which can cause saturation in the central parts of the image. To lessen this effect masking was added to the back window of the injector in a small strip along the centerline. Masking was also added to cover the sections of the window not directly behind the injector.

THEORETICAL DEVELOPMENT: GENERAL MECHANISM OVERVIEW

In this theory the atomization of the swirling liquid film is accomplished by stripping small bits of mass off of disturbances on the film's surface. The process starts with the initiation of a disturbance followed by the growth of the disturbance, the stripping of a small bit of the protuberance, the regrowth of the disturbance and another stripping event. The regrowth-stripping cycle continues until the disturbance exits the injector. By assuming that stripping occurs when the forces on the atomized section are balanced, an entrained volume per disturbance can be calculated. This volume is found by solving the force-balance equation, over the atomized section, for the height of the stripped portion. The forces are balanced along the direction of separation which is generally not the horizontal or vertical direction. Figure 3 illustrates the forces acting on an atomizing section of a disturbance. Lumping the trigonometric terms and force-proportionality constants together for each force and nondimensionalizing by an approximation of the liquid's inertial force, $\rho_l \tau_g^2 v_{in}^2$, the force balance equation for the state shown in Fig. 3 is

$$\Phi\left[C_{L/D}\, A_{cs} / \tau_{gap}^2 + C_f \left(v_{g,recirc} / v_g\right)^2 \left(A_{surface} / \tau_{gap}^2\right)\right] - C_c\, V_{entrained} v_{local,\theta}^2 / \left(r_{rotate} \tau_{gap}^2 v_{in}^2\right)$$
$$- C_\sigma We_\ell\, A_{annular} / \left(R_{curvature} \tau_{gap}\right) - C_\mu\, A_{surface} v_g / \left(Re_\ell v_{in} \tau_{gap} \delta\right) = 0$$

where Φ is the momentum-flux ratio of the gas and liquid at inlet conditions ($\rho_g v_g^2 / \rho_l v_{in}^2$), $We_\ell = \sigma / \left(\rho_\ell \tau_{gap} v_{in}^2\right)$ is the liquid Weber number and the Reynolds number of the liquid is $Re_\ell = \rho_\ell \tau_{gap} v_{in} / \mu_\ell$. Here gravity has been neglected, but can easily be added as long as the general direction (i.e., whether it aids or hinders breakup) is known. In the vast majority of cases, especially in rocket engines, the gravity term is not important. As long as the separation angle does not approach 0 or 90°, the proportionality constants for each term may be considered O(0.1) to O(1), depending on the stripping angle. The areas, radius of curvature and entrained volume all depend on the disturbance shape and, in general, are functions of the height of the atomized section, δ. Solving for the above equation for δ and using that value in the entrained volume relation provides a value for the volume of liquid atomized from *each* disturbance during a *single* atomization event. The atomization rate for the single disturbance is the entrained volume divided by an atomization time. An atomization time can be determined based on the growth rate of a disturbance and a stripping time, considered to be the time it takes the gas to flow over the atomizing section.

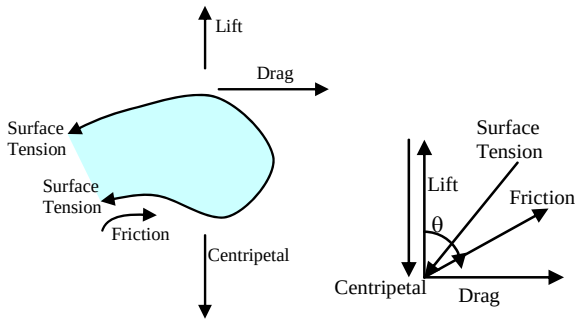

Figure 3: A depiction of the forces acting on the separating portion of a disturbance

Several disturbances may be present on the film at any time. One must calculate and account for the total number of disturbances present on the film to get the total atomization rate. Since disturbances can be caused by many initiating mechanisms, e.g. liquid turbulence or hydrodynamic instabilities, there may be multiple types of disturbances present on the film. The types and numbers of each disturbance are dependent on the geometry and operation of the injector. A review of general atomization mechanisms can aid in the determination of which initiating mechanisms are present for a given injector [1]. The atomization rate, found from the entrained volumes and atomization times, must be considered for each type of disturbance present. The overall atomization rate is considered to be the sum of the atomization rates for each type of disturbance. In many instances simplified calculations or general examinations will reveal that while several types of disturbances are present, only a one or two make significant contributions to the atomization rate.

The atomization efficiency is found by comparing the volumetric flow rate of the incoming liquid with the atomization rate from all disturbances. In most cases, a film length is needed to arrive at the total number of disturbances. To get the correct atomization rate, the correct film length must be used. This film length is unknown at the start of the calculations and must be estimated. If the atomization rate calculated from the estimated film length is not equal to the inlet flow rate then the film length is incorrect and a revised estimate for the film length should be used to get a new atomization rate. This iteration process continues until the two flow rates are equal. Note, however, that the film length cannot exceed the atomizer length as this theory is built on the assertion that atomization occurs from a film only. Once the correct film length has been determined then the atomization efficiency can be calculated as[3] $\eta_{atom} = \left(L_{inj} - L_{film}\right)/L_{inj}$.

In addition to atomization efficiency, the atomized portion height allows a primary droplet diameter to be estimated. Assume the stripped portion of each disturbance initially forms a ligament whose length is that of the disturbance. The ligament diameter is related to this length and the atomized volume, $d_{lig} = \sqrt{V_{en}/\left(\pi L_{lig}\right)}$. This ligament breaks up into droplets via the Rayleigh mechanism creating roughly $N_{drop} = 6V_{en}/\left\lfloor \pi\left(1.89 d_{lig}\right)^3 \right\rfloor$ droplets with a diameter of $d_{drop} = \left[6V_{en}/\left(\pi N_{drop}\right)\right]^{1/3}$. The average droplet diameter produced in the injector is the weighted average (with droplet number) of the diameters produced by each type of disturbance present in the injector.

A summary of the steps taken to determine atomization rate and primary droplet diameter are given in Table 1.

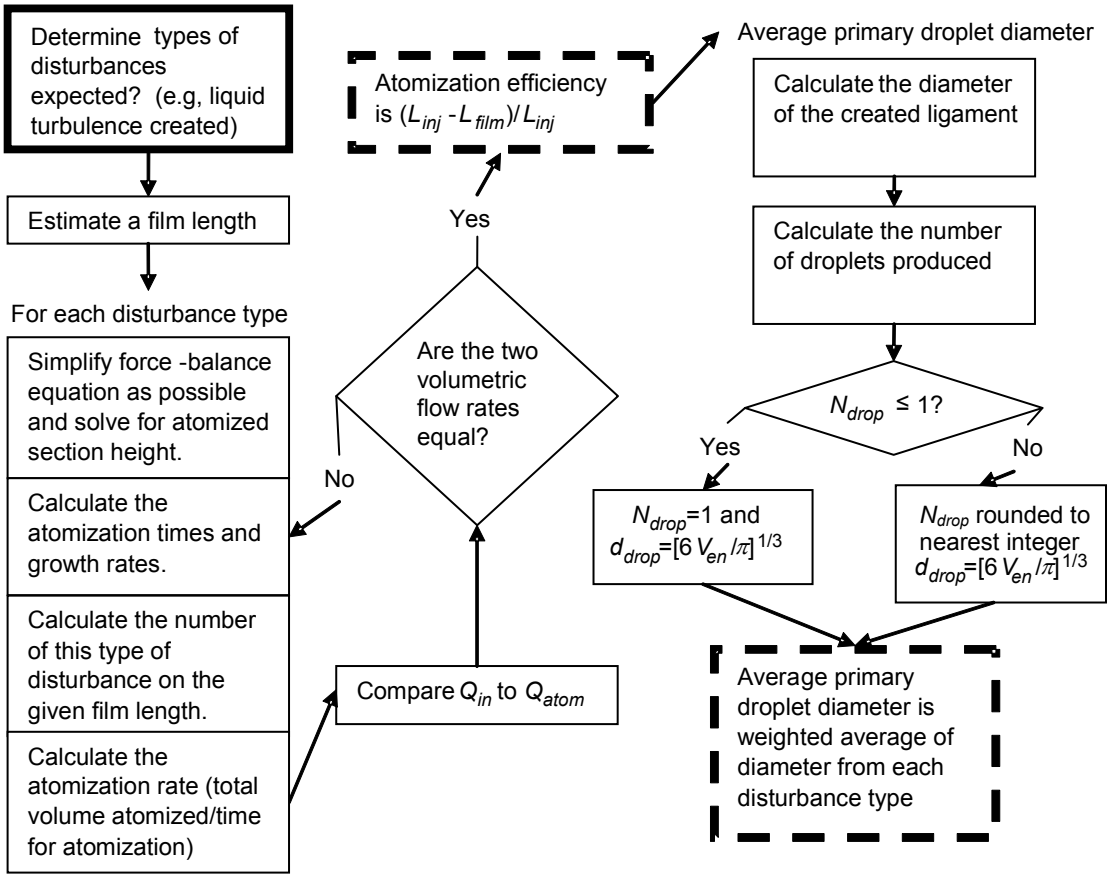

Table 1: A summary of the basic process for determining atomization efficiency and average droplet diameter.

RESULTS AND DISCUSSION: APPLICATION TO A GAS-CENTERED SWIRL-COAXIAL INJECTOR

Here some details of application are given for the injector of interest: a gas-centered swirl coaxial injector illustrated in Fig. 1 and described in the introduction. The velocities that appear in the force-balance equation are related to the geometry of the injector and appropriate methods for determining these velocities are discussed first. A review of film-atomization literature suggests there are four main disturbance causes in films undergoing stripping[1]. These are initiated by liquid turbulence, hydrodynamic instabilities, coherent gas-phase structures (here, mainly recirculation zones following gas-flow separation) and gas-phase turbulence. Following the velocity discussion, each type of disturbance will be examined for importance and likelihood under typical operating conditions as given in Table 2. Shape approximations needed to calculate areas, radii of rotation and curvature and entrained volume will also be presented.

Gap Thickness (in)	0.065
Outlet Radius (in)	0.375
Liquid Mass Flow (lb/s)	0.101
Gas Mass Flow (lb/s)	0.135
Liquid inlet velocity (ft/s)	19.1
Gas inlet velocity (ft/s)	~1100

Table 2: Operating conditions for the GCSC injector. Working fluids are gaseous nitrogen and water; test conducted at STP.

One set of information that depends on the specific injector (and is often not fully known) are the relative and liquid-tangential velocities. The gas velocity, which is purely axial in a GCSC injector, is much greater than the liquid velocity. Therefore, assume the bulk relative velocity is also purely axial and equal to the gas velocity. Earlier work on a similar injector suggested that the appropriate gas velocity is not its bulk velocity but its value near the interface which can be approximated from a single-phase numerical simulation of the injector[3]. The relative velocity of recirculating gas, important in the friction term, arises from turbulent eddies or other recirculation zones and can be estimated from such sources as turbulent statistics (the root-mean-square velocity fluctuation in the axial direction) or flow simulations. Multiphase, VOF simulations (see Fig. 4) suggest that the liquid-tangential velocity falls sharply following liquid injection and that the ratio of tangential to inlet velocity is O(1); an initial approximation might assume $v_{local,\theta}=C_{\theta}v_{in}$. From simulations a more accurate functional dependence between the two velocities could be developed; however, these simulations are quite time consuming and given the other assumptions, unlikely to appreciably improve accuracy.

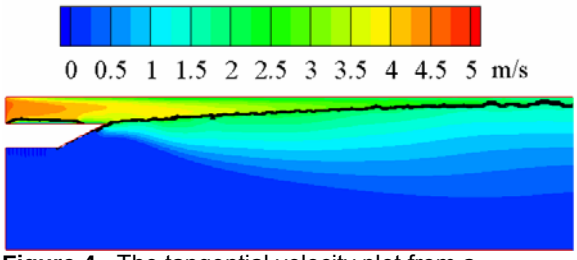

Figure 4: The tangential velocity plot from a simulation with a gas velocity ~350 ft/s. The black line represents the approximate location of the interface

Due to the amount of kinetic energy in the gas, any ligaments created by liquid turbulence would rapidly collapse into the liquid, likely before they reach a height where appreciable stripping can occur. To confirm this consider a limit to the untoppled ligament length by assuming the ligament starts to topple once the torque exerted by drag on a ligament is exactly counterbalanced by the inertial force maintaining the ligament's upright position[5]. The limit to the ligament length would, therefore, be roughly $L\sim(\rho_g/\rho_l)(v_{rel}/v_{lig,x})(D_{lig}/\tau_{gap})\tau_{gap}$. Sarpkaya and Merrill[5] made measurements of D_{lig}/τ_{gap} for films with no imposed gas flow and reported a value of approximately 0.4. Their films were more than three times the thickness found in the current injector and did not include swirl, so this cited value is expected to be somewhat larger than the actual value in the current study, but can serve as an upper bound. Using 0.4 for D_{lig}/τ_{gap} suggests a maximum ligament height of $O(10^{-2})$ inches—the ligament would be approximately the same height and width. Considering a force balance where only surface tension impedes atomization and approximating the disturbance as a right circular cylinder, the stripped portion of this ligament would be $O(10^{-8})$ inches high with a volume $O(10^{-12})$ in^3. Even if the entire surface area of the film were occupied with ligaments of that diameter, less than 200 ligaments would be present at a given time. Two hundred ligaments atomizing $O(10^{-12})$ in^3 each would atomize 0.006% of the total film. Even if the estimated ligament length is off by an order of magnitude, the result still indicates that liquid-turbulence-induced disturbances contribute very little, if at all, to the overall atomization.

To study the importance of hydrodynamic instabilities on the film surface, the stability of the film must be considered. The inviscid, linear analysis of Ibrahim and Jog[2] for swirling sheets of finite thickness is an appropriate starting point for estimating the stability of the film. Modifications to this theory should be made to account for the wall instead of a gas flow on the outer boundary of the liquid. Another approach is to measure the wavelength of instabilities observed in experiments and simulations and use this value as an estimate; growth rates may also be available from the data, but they are more difficult to measure than the wavelengths. The force-balance equation was solved for a range of heights and wavelengths at the conditions listed in Table 2. The most accurate geometry is likely to be sinusoidal, but the surface area and volume calculations for an annular, sinusoidal wave are rather complex; consequently, the calculations were performed by assuming the atomizing section was parabolic in cross section and still annular in nature. The results reveal a minimum wave height which must be achieved before atomization occurs. For the examined conditions this height is roughly that of the separating lip. Typical growth rates for annular sheets[2] suggest that over the 1.5 inches of the injector outlet only a small number of waves, less than five and possibly none, would reach a sufficient height for atomization. The calculations indicate that each wave would lose, at most, a volume equivalent to ~2.5% of the total film volume (if the film length is that of the injector). Consequently, the injector must be very long or other atomization mechanisms unimportant before hydrodynamic waves play a significant role. Indeed, experimental results show coherent waves exist only at operating conditions where little film atomization occurs. One final note is that centripetal forces play an important role with atomization from these waves due to their height when atomization occurs; the other forces cannot be neglected, however. An experimental picture showing evidence of hydrodynamic instabilities is presented in Fig. 5; under the operating conditions in which these waves are visible (lower gas velocities than given in Table 2), a sheet is formed downstream of the injector exit with only a small amount of atomization occurring from the wall-bound film. These results reinforce the finding that hydrodynamic instabilities do not play a major role in atomization when the entire film is atomized, but they may be important in situations where atomization from both the film inside the injector and sheet downstream of the injector exit are important.

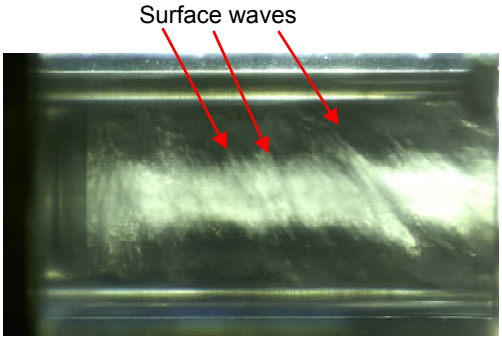

Figure 5: Experimental photograph where surface waves are highlighted with arrows. Flow is from left to right.

Large-scale gas-phase structures may occur in the current configuration as a result of flow separation at the lip which initially separates the two phases. Simulations and experiments show that this separation produces a raised disturbance on the film surface just downstream of the lip. Atomization may occur from the top of this raised “bump”. The simulations also show that the bump shape is asymmetric with a steep boundary marking its upstream edge and a gradual, almost linear fall-off downstream from its apex. For simplicity, however, the atomizing section of this disturbance may be approximated as symmetrical and parabolic in shape. An examination of the problem suggests that in this situation drag and friction actually oppose one another instead of aiding each other. In the force balance given above, however, both lift and friction forces are positive because they were considered to aid each other, as shown in Fig. 3. Indeed, the simulations (Fig. 6) show nearly horizontal deformation of the disturbance occurs with friction pulling the liquid upstream while drag is pushing it downstream. Trigonometric parameters relating the angles of the forces and stripping are buried in the constants of each term of the force-balance equation; in the case where stripping is nearly horizontal or vertical some of these constants become very small. The axial nature of the actual deformation and the radial nature of the centripetal force term suggest, then, that this force may be neglected. Simulations show that the friction force dominates, which causes the atomized section to be pulled upstream where most of this atomized section is redeposited into the bulk film (see Fig. 6). Consequently, it appears that the recirculation zone is not very important in producing droplets via stripping.

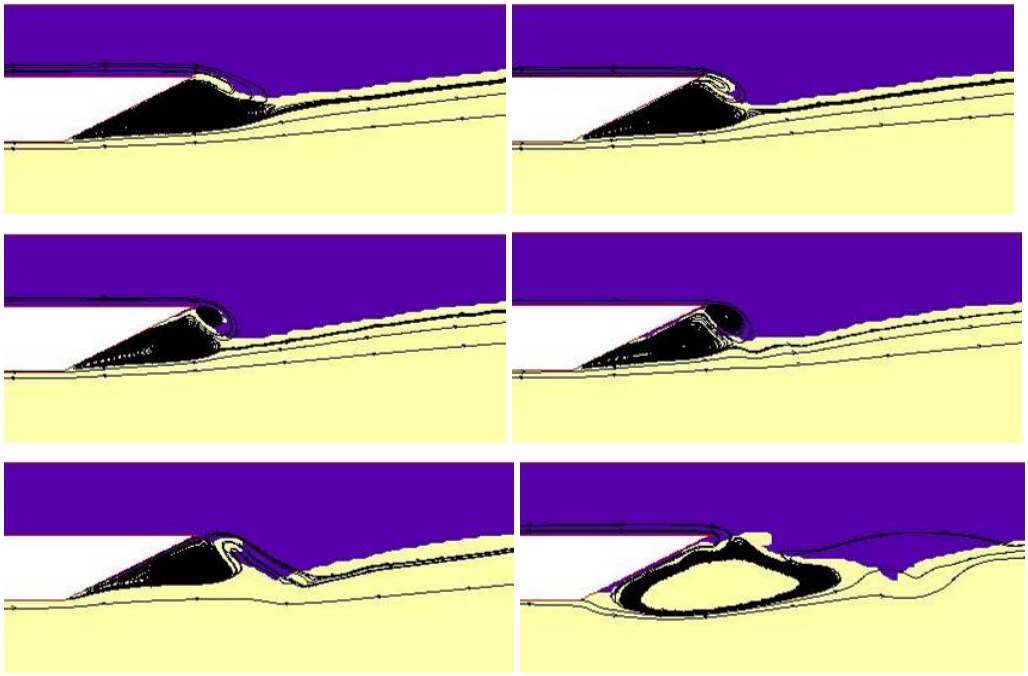

Figure 6: A series of pictures from the multiphase simulations showing the evolution of the bump. From left to right, top to bottom the pictures show a progression of 0.06 s (0.012 s intervals) of the bump's life. A close-up of the injector, just at the separating lip is shown; in this simulation, a tapered lip was used. The liquid is blue, the gas is yellow, the separating lip is white and the black lines are streamlines.

The recirculation zone undergoes a complex behavior which causes it to collapse, however. This collapse causes the "bump" to move rapidly downstream; the rapid exist of this bump is observed in the experimental results where it causes a pulse of droplets when the "bump" reaches the exit of the injector. The collapse of the recirculation zone is caused by the interplay between the primary and secondary zones and their distortion of the liquid. The two zones pull small cusps of the film towards each other slowly isolating the secondary zone from the primary one—decreasing energy input into the secondary zone until it weakens and collapses. The collapse of the secondary zone leads to collapse/shedding of the primary zone which, in turn, leads to a large pulse of exiting liquid. So, while likely unimportant when anchored, the "bump" may contribute to atomization as it exits the injector. The current theory does not address the atomization of the bulk of this pulse, however, as it breaks up at or after the atomizer exit, perhaps as it attempts to negotiate the corner there. The theory can give insight into the bump-shedding process, however.

Gas-phase turbulence may cause distortions on the film surface in ways similar to liquid turbulence provided that the gas-phase eddies have sufficient energy. In order to distort the interface the energy of the turbulent eddy must exceed the surface energy of the film. Mathematically, this condition yields a criterion that $d_{eddy} \gtrsim \sigma/\rho_g v_{eddy}^2$.[6] If the eddies responsible for disturbance formation lie in the inertial range as they do for liquid turbulence then $v_{eddy} \sim v_{rms}(d_{eddy}/d_l)^{1/3}$ where the root-mean-square velocity is in the cross stream direction and d_l is the integral length scale, $d_H/8$.[6] Eddies responsible for atomization therefore meet the following criterion, at a minimum, $d_{eddy}/d_H = C_{eddy}(\sigma/\rho_g d_H v_{eddy}^2)^{3/5} = C_{eddy} We_{dH,eddy}^{3/5}$ with the proportionality constant O(1). Turbulence data either from an injector experiment or from fully developed pipe flow can be used to

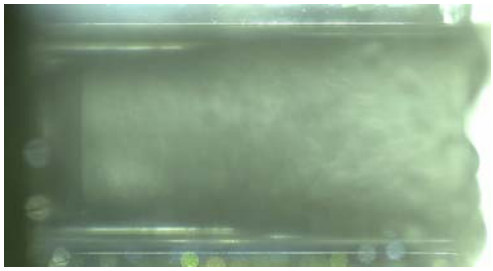

Figure 7: A sample photograph from the experiments showing the chaotic surface associated with operating conditions with good atomization. Flow moves from left to right.

determine the percentage of eddies capable of producing atomization as well as an average eddy size for atomization. Experimental results show the film is increasingly "opaque" as the gas velocity increases. This increase in opacity suggests that the surface is scattering more light—that the surface is rougher and more chaotic (see Fig. 7). While still preliminary, these findings indicate that the film's surface is very turbulent. Earlier discussion suggests liquid turbulence is an unlikely source of atomization. Arguments that the gas turbulence is the more important of the two are supported by experimental findings that increases in opacity are more evident with increases in the gas velocity than with increases in liquid velocity. Calculations based on the values given in Table 2 predict primary droplet diameters of $O(10^{-2})$ to $O(10^{-3})$ inches. Downstream droplet measurements, i.e. measurements after secondary breakup has occurred, of $2x10^{-4}$ to $3x10^{-3}$ inches were made in similar injectors operating at increased pressures[3]. This finding also suggests gas-phase turbulence plays an important role in atomization at operating conditions with good atomization. The shape of disturbances caused by gas-phase turbulence is unknown; yet, an assumption of the process involved gives some suggestions. It is theorized that the rotating vortices contact the surface and are energetic enough to distort it causing a divot. Due to their rotation these vortices pull liquid up along their periphery as a rotating roller would in dip coating. Atomization theories involving liquid turbulence often assume a roughly spherical shape for vortices [6] and work on the coherent structures of turbulence suggest a straight or curved cylindrical shape [7]. A simple approximation would be cylindrical vortices with a length equivalent to the circumference of the upward rotating hemisphere if they were spherical, i.e. πR_{eddy}. A rough resulting disturbance shape is given in Fig. 8.

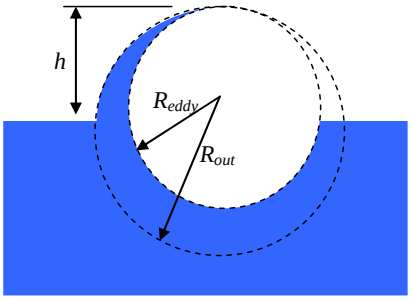

Figure 8: Approximate disturbance shape caused by gas-phase turbulence

Considering the four types of disturbance-creation mechanisms it appears that gas-phase turbulence is the most important in situations where the entire film is atomized within the injector cup. Calculations involving gas-phase turbulence also give reasonable results which are in a range expected from earlier experimental results. At lower momentum-flux ratios and/or lower gas velocities where gas-phase turbulence lacks the energy to appreciably distort the film surface, hydrodynamic instability waves are likely important. At very low gas velocities, liquid turbulence may also be important[5, 6]. Experimental results show coherent wave-like structures at low gas velocities when atomization is poor and a sheet exists downstream of the injector exit supporting the findings of the importance of hydrodynamic instabilities at low momentum flux ratio. As the gas velocity increases, an increase in opacity indicating a rougher and more chaotic surface is observed indicating the increased importance of gas-phase turbulence. Considering one or two disturbance types greatly eases the application of the theory. Further simplifications based on exact operating conditions, and the resultant relative magnitudes of various forces, are also possible.

CONCLUSIONS

A theory has been developed which uses an understanding of general atomization mechanisms to calculate atomization properties of injectors utilizing wall-bounded films. A general outline of the process was given as well as some discussion of its application to a gas-centered swirl-coaxial injector. The theory assumes that atomization occurs through a process of surface disturbance creation followed by the gas-phase initiated stripping of a portion of these disturbances. Stripping occurs when the forces acting on a small section of a disturbance are balanced. This small section separates from the bulk fluid forming a ligament and, eventually, droplets. Application of the theory requires several assumptions, specifically determining velocities, disturbance causes and disturbance shapes. A discussion of velocity determination suggests that simple single-phase simulations are an ideal way to affordably estimate most of the gas velocities found in the theory. The model is applicable to any number of disturbance creation mechanisms; however, examination indicates that one, that due to gas-phase turbulence, is the likely cause of atomization under ideal operation of the gas-centered swirl-coaxial injector studied. Disturbance shapes needed for application of the theory can often be estimated rather accurately by considering the creation method of the disturbance, i.e. the disturbance type. Overall, the theory is powerful in its ability to offer predictions for a wide range of injectors operating over a wide range of conditions, and preliminary

experimental results back-up the theory's potential for prediction of GCSC atomization. Both suggest gas-phase turbulence is of primary importance.

A large amount of future work is planned. Much work is needed to validate this model and find suitable ranges for the constants contained within it. Film length, droplet size predictions and scaling with operating pressure and injector size are currently planned as points for validation. Simulations and experimental work will be coupled to anchor and improve velocity assumptions. Sensitivity of the theory to various operating parameters and assumptions will also be explored.

NOMENCLATURE

A	Area
C	constant
d	diameter
L	length
N	number of things
r,R	radius
Re	Reynolds number
v	velocity
V	volume
We	Weber number
δ	height of atomized portion of the disturbance
η	efficiency
μ	viscosity
ρ	density
σ	surface tension
τ	thickness
Φ	momentum-flux ratio

Subscripts

atom	atomization
cs	cross-section
curv	curvature
disturb	disturbance
drop	droplet
eddy	turbulent eddy
en	entrained
f	friction
g	gas
gap meet	of the gap prior to where the liquid and gas
in	inlet value of liquid
inj	injector
l	liquid
L/D	Lift and Drag
lig	ligament
recirc	recirculation
rot	rotation
o	outlet of the injector
z	in the axial direction
μ	viscous
θ	in the angular direction
σ	surface tension

ACKNOWLEDGEMENTS

Experimental support and assistance was rendered by Randy Harvey of ERC Corporation.

BIBLIOGRAPHY

[1]Lightfoot, M. D. A., "Atomization of Wall-Bounded Two-Phase Flows", submitted *Atomization Spray*, 2006.

[2]Ibrahim, A. A. and Jog, M. A., "Effect of Liquid and Air Swirl Strength and Relative Rotational Direction on the Instability of an Annular Liquid Sheet", *Acta Mech*, vol. 186, pp. 113-133, 2006.

[3]Strakey, P.Cohn, R. K. and Talley, D. G., "The Development of a Methodology to Scale between Cold-Flow and Hot-Fire Evaluations of Gas-Centered Swirl Coaxial Injectors", 52nd JANNAF Propulsion Meeting, Las Vegas, NV, May 10-14, 2004.

[4]Lightfoot, M. D. A.Danczyk, S. A. and Talley, D. G., "Atomization in Gas-Centered Swirl-Coaxial Injectors", 19th Annual Conference on Liquid Atomization and Spray Systems, Toronto, ON, May 23-26, 2006.

[5]Sarpkaya, T. and Merrill, C. F., "Spray Generation from Turbulent Plane Water Wall Jets Discharging into Quiescent Air", *AIAA J*, vol. 39, no. 7, pp. 1217-1229, 2001.

[6]Sallam, K. A. and Faeth, G. M., "Surface Properties During Primary Breakup of Turbulent Liquid Jets in Still Air", *AIAA J*, vol. 41, no. 8, pp. 1514-1524, 2003.

[7]Alfondi, G., "Coherent Structures of Turbulence: Methods of Eduction and Results", *Applied Mechanics Reviews*, vol. 59, pp. 307-323, 2006.